ACOUSTICS 2012

Reduced order model for noise and vibration attenuation of water immersed viscoelastic sandwich structures

L. Rouleau[a], J.-F. Deu[a], A. Legay[a], J.-F. Sigrist[b] and P. Marin-Curtoud[c]

[a]Laboratoire de Mécanique des Structures et des Systèmes Couplés, 292, rue Saint Martin 75141 Paris Cedex 03
[b]Département Dynamique des Structures, CESMAN, DCNS research, Indret, 44620 La Montagne, France
[c]DGA Techniques Navales, BP 40915, 83050 Toulon Cedex, France
lucie.rouleau@cnam.fr

The structural optimisation of structures with constrained viscoelastic layers is a major issue in the design of submarines, to assure stealthiness performances. This work proposes reduction methods to solve the system composed of a mechanical structure with embedded viscoelastic material coupled to fluids in the frequency domain. These numerical strategies are applied to the response of a bidimensional sandwich ring coupled to external fluid ; and extended to a tridimensional structure.

1 Introduction

Viscoelastic damping is a common technique in industrial applications to reduce the vibrations of a structure and to control the level of noise. In naval shipbuilding, it has been used since the 1960s to enhance submarine stealthiness performance. The viscoelastic material is generally embedded in the structure as a constrained layer since damping is proportional to shear stress. During the design process of some particular parts of a submarine, engineers have to optimize the position and the material parameters of this viscoelastic layer. In order to evaluate acoustic radiation of the submarine, the external fluid has to be taken into account and coupled to the vibrating structure with viscoelastic treatment. The goal of this work is to present reduction methods to calculate the frequency response of the sandwich structure with viscoelastic core, coupled to fluid. Several reduction methods are tested on a bidimensional structure. The strategy is then extented to a tridimensional structure.

2 Description of the bidimensional structure

A bidimensional ring made of steel with partial viscoelastic core and radial stiffeners in steel, immersed into water is considered. The model, shown in Figure 1, is fixed at the intersection of the stiffeners and a unit radial load is applied at the left part of the structure.

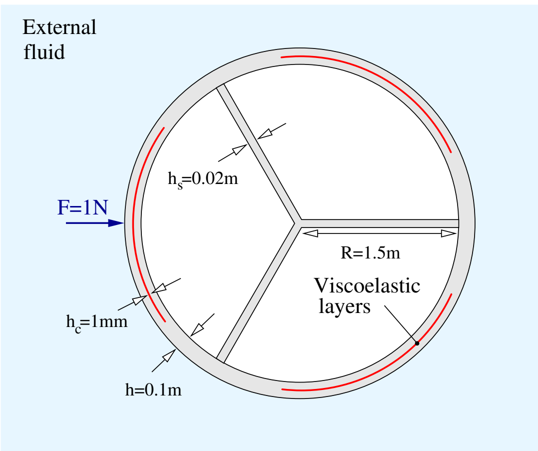

Figure 1: Description of the studied problem

The viscoelastic layer is made of Paulstra's Deltane 350 whose shear modulus and loss factor are represented as a function of frequency on Figure 2. The expression of the complex shear modulus describing the frequency dependence of the viscoelastic material's properties is given by a fractional Zener model :

$$G^*(\omega) = \frac{G_0 + G_\infty (\mathrm{i}\omega\tau)^\alpha}{1 + (\mathrm{i}\omega\tau)^\alpha} \qquad (1)$$

The relaxed and unrelaxed moduli G_0 and G_∞, the relaxation time τ and the order of the derivation α are identified from the experimental master curves of Deltane 350 at 12^{o}C (Figure 2) :

$$G_0 = 1.88 \text{ MPa}, \quad G_\infty = 0.78 \text{ GPa}, \quad \tau = 0.15\ 10^{-6} \text{ s}, \quad \alpha = 0.5$$

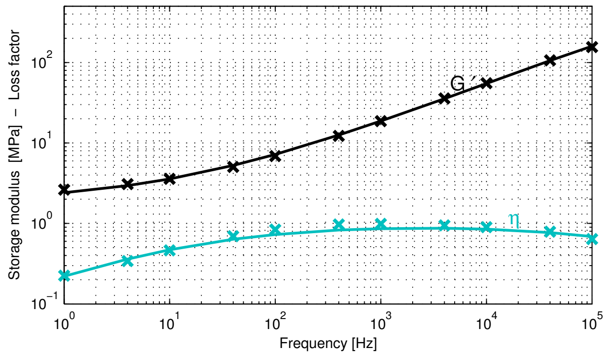

Figure 2: Master curves of Deltane 350 at 12^{o}C (crosses : experimental datas, line : fitted results)

The structure is meshed with plane stress 2-node beam elements with 4 degrees of freedom per node, as in [1]. This element is based on 'zigzag' theories : Timoshenko assumptions are made for the viscoelastic core, while Bernoulli assumptions are taken for the elastic faces.

The mechanical displacement field within the ith layer is written in the local coordinate system (x, z) :

$$u_{xi}(x,z,t) = u_i(x,t) - (z - z_i)\theta_i(x,t) \qquad (2)$$
$$u_{zi}(x,z,t) = w(x,t)$$

where u_{xi} and u_{zi} are the axial and transverse displacement, $i = a, b$ for the upper and lower faces and $i = c$ for the core, u_i and θ_i are the axial displacement of the centre line and the fibre rotation of the ith layer, and w is the transverse displacement. Due to the kinematics of the sandwich beam, they can be written in terms of $\bar{u}$, w' and $\tilde{u}$, (see details in [2]) as defined by :

$$\bar{u} = \frac{u_a + u_b}{2}, \qquad \tilde{u} = u_a - u_b, \qquad w' = \frac{\partial w}{\partial x} \qquad (3)$$

The axial displacement is discretized with linear shape functions while cubic shape functions are used for the deflexion. The interpolation matrix $\mathbf{N}$ relates the generalized displacements $\mathbf{d}^e = [\bar{u}, w, \tilde{u}]^T$ to the elementary degrees of freedom $\mathbf{q}^e = [\bar{u}_1, w_1, w'_1, \tilde{u}_1, \bar{u}_2, w_2, w'_2, \tilde{u}_2]^T$: $\mathbf{d}^e = \mathbf{N}\mathbf{q}^e$. With this discretization, the governing equation becomes :

$$\left[-\omega^2 \left(\mathbf{M}_a + \mathbf{M}_b + \mathbf{M}_c\right) + \left(\mathbf{K}_a + \mathbf{K}_b + \mathbf{K}_c^*(\omega)\right)\right] \mathbf{q} = \mathbf{F}^e \qquad (4)$$

where $\mathbf{M}_i$ and $\mathbf{K}_i$ $(i = a, b, c)$ are the global matrices obtained by assembling the element matrices $\mathbf{M}_i^e$ and $\mathbf{K}_i^e$ of each layer, given by :

$$\mathbf{M}_i^e = \int_0^{L_e} \rho_i A_i \left(\mathbf{N}_{xi}^T \mathbf{N}_{xi} + \mathbf{N}_z^T \mathbf{N}_z + \mathbf{N}_{ri}^T \mathbf{N}_{ri}\right) \mathrm{d}x, \qquad (5)$$
$$i = a, b, c$$

$$\mathbf{K}_f^e = E_f \left(A_f \int_0^{L_e} \mathbf{B}_{mf}^T \mathbf{B}_{mf} \mathrm{d}x + I_f \int_0^{L_e} \mathbf{B}_{bf}^T \mathbf{B}_{bf} \mathrm{d}x \right), \qquad f = a, b \tag{6}$$

$$\mathbf{K}_c^e = G_c^*(\omega) \left[2(1+\nu) \left(A_c \int_0^{L_e} \mathbf{B}_{mc}^T \mathbf{B}_{mc} \mathrm{d}x + I_c \int_0^{L_e} \mathbf{B}_{bc}^T \mathbf{B}_{bc} \mathrm{d}x \right) + k_c A_c \int_0^{L_e} \mathbf{B}_{sc}^T \mathbf{B}_{sc} \mathrm{d}x \right] \tag{7}$$

where L_e is the length of the physical element e, ρ_i, E_i, A_i and I_i are respectively the density, the Young modulus, the section, and the moment of inertia of the ith layer. G_c and k_c are the shear modulus and the shear correction. The line matrices $\mathbf{N}_{xi}$, $\mathbf{N}_z$, $\mathbf{N}_{ri}$, $\mathbf{B}_{mi}$, $\mathbf{B}_{bi}$ and $\mathbf{B}_{sc}$ are directly linked to the interpolation matrix $\mathbf{N}$. For convinience, the stiffness and mass matrices of the structure are denoted $\mathbf{K}_{\mathrm{S}}^*(\omega)$ and $\mathbf{M}_{\mathrm{S}}$, with $\mathbf{K}_{\mathrm{S}}^*(\omega) = \mathbf{K}_a + \mathbf{K}_b + G_c^*(\omega)\mathbf{K}_c$ and $\mathbf{M}_{\mathrm{S}} = \mathbf{M}_a + \mathbf{M}_b + \mathbf{M}_c$. The effect of the external fluid on the structural vibrations is taken into account through an added mass matrice. An analytical solution for the pressure field exists for a water-submerged bidimensional circular shape body. This solution is obtained by expressing the radial displacement of the structure and the external pressure in the fluid as Fourier series. An added mass operator for the external fluid, denoted $\mathbf{M}_{\mathrm{F}}^{\mathrm{a}}$, is thus derived from the coupling term of the governing equations of the coupled system, as described in [3].
The system to be solved is :

$$\left[\mathbf{K}_{\mathrm{S}}^*(\omega) - \omega^2 (\mathbf{M}_{\mathrm{S}} + \mathbf{M}_{\mathrm{F}}^{\mathrm{a}}) \right] \mathbf{u} = \mathbf{F} \tag{8}$$

where $\mathbf{K}_{\mathrm{S}}^*(\omega)$ is the frequency-dependent stiffness matrix of the structure with viscoelastic layer, $\mathbf{M}_{\mathrm{S}}$ is the mass matrix of the structure, and $\mathbf{M}_{\mathrm{F}}^{\mathrm{a}}$ the added mass matrix due to the presence of external fluid.

3 Numerical results of the bidimensional structure

The frequency response of the structure with viscoelastic layer, coupled to the external fluid at the excitation point can be obtained by a direct method which consists in solving Eq.8 for each frequency (Figure 3). On this figure, the two results corresponding to the undamped sandwich structure ($G = G_0$) and the damped one ($G = G^*(\omega)$) are presented. The viscoelastic treatment results in a significant reduction in the displacement levels.

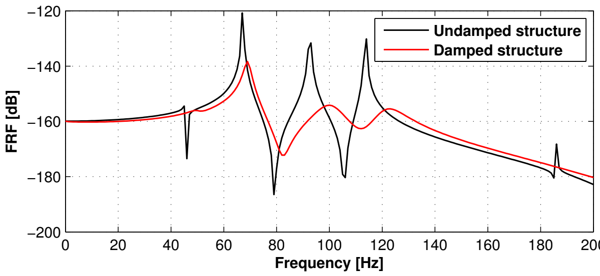

Figure 3: Direct frequency response of the structure

The pressure in the fluid is calculated at a given frequency from the corresponding displacement of the structure using the analytical relationship between the fluid pressure and the Fourier coefficients of the radial displacement in the adopted modelling of the external fluid (see [3] for details). Figure 4 shows that the fluid can be taken incompressible as both compressible and incompressible hypothesis lead to similar levels of pressure in the external fluid. Therefore, in the sequel, the fluid is taken as incompressible.

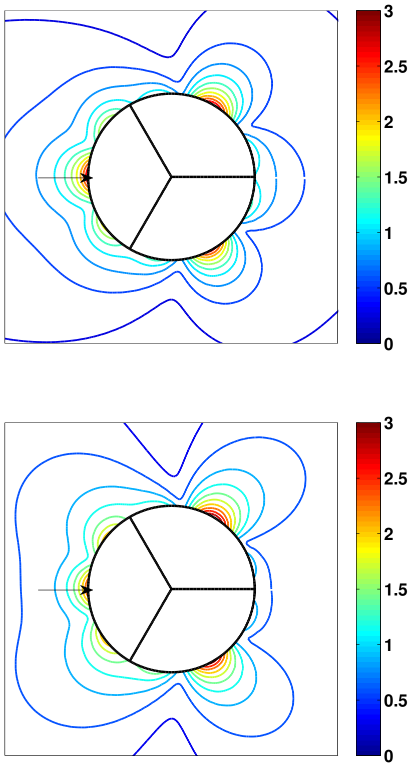

Figure 4: Pressure field in the external fluid at f = 100 Hz for an incompressible (top) and compressible (bottom) hypothesis for the external fluid.

For larger models, the calculation of the frequency response is time consuming as the stiffness matrix needs to be evaluated at each frequency and the added mass matrices are full: reduction methods are thus of great help.
Most reduction techniques are based on Ritz approximation which consists in assuming that the full order degrees of freedom $\mathbf{u}$ can be estimated by a linear combination of well chosen independent vectors $\mathbf{T}_i$:

$$\mathbf{u} = \mathbf{T}\mathbf{q} \tag{9}$$

where $\mathbf{q}$ is the reduced order degrees of freedom. The reduced system is then obtained by projecting Eq. 8 on the reduction basis :

$$\left[\mathbf{T}^{\mathrm{T}} \mathbf{K}_{\mathrm{S}}^*(\omega) \mathbf{T} - \omega^2 (\mathbf{T}^{\mathrm{T}} \mathbf{M}_{\mathrm{S}} \mathbf{T} + \mathbf{T}^{\mathrm{T}} \mathbf{M}_{\mathrm{F}}^{\mathrm{a}} \mathbf{T}) \right] \mathbf{q} = \mathbf{T}^{\mathrm{T}} \mathbf{F} \tag{10}$$

3.1 Modal projection

The usual reduction basis of a modal projection consists of low frequency normal modes ($\boldsymbol{\phi}_i$) and a static correction $\mathbf{T}_{\mathrm{s}}$ to account for high frequency modes :

$$\mathbf{T} = [(\boldsymbol{\phi}_i^*) \ , \ \mathbf{T}_{\mathrm{s}}] \tag{11}$$

where $\left(\boldsymbol{\phi}_i^*\right)$ are solution of

$$\left[\mathbf{K}_{\mathrm{S}}^*(\omega_i) - \omega_i^2 \left(\mathbf{M}_{\mathrm{S}} + \mathbf{M}_{\mathrm{S}}^{\mathrm{a}} \right) \right] \boldsymbol{\phi}_i^* = \mathbf{0} \tag{12}$$

and the static correction corresponds to the static solution to the load evaluated at a high frequency modulus

$$\mathbf{T}_s = \mathbf{K}^{-1}_{S_{|(\omega=\omega_c)}} \mathbf{F}. \tag{13}$$

The computation time of complex damped modes by iterative algorithms is generally not compensated by the advantages of using reduction techniques. Therefore, real projection basis are usually looked for. For structures with low damping, considering real undamped modes in the modal reduction basis can give fair results :

$$\mathbf{T}_1 = [(\boldsymbol{\phi}_i)\ ,\ \mathbf{T}_s] \tag{14}$$

$$\left[\mathbf{K}^0_S - \omega_i^2 \left(\mathbf{M}_S + \mathbf{M}^a_S\right)\right] \boldsymbol{\phi}_i = \mathbf{0} \tag{15}$$

with $\mathbf{K}^0_S = \Re(\mathbf{K}^*_S(\omega = 0))$. However, for highly damped structures, the real undamped modes are not sufficient to account for the frequency shift induced by the high dependency on frequency of the material properties. Several approaches are possible for the construction of an enriched reduction base efficient for highly damped structures : use of normal pseudo-modes, multi-model, introduction of residual [4]. The multi-model approach is adopted here. It consists in adding a set of real normal modes associated with a stiffness matrix calculated at a high frequency modulus $G^*(\omega_c)$, $(\boldsymbol{\psi}_i)$:

$$\mathbf{T}_2 = [(\boldsymbol{\phi}_i)\ ,\ (\boldsymbol{\psi}_i)\ ,\ \mathbf{T}_s] \tag{16}$$

$$\left[\Re(\mathbf{K}^*_{S_{|(\omega=\omega_c)}}) - \omega_i^2 \left(\mathbf{M}_S + \mathbf{M}^a_S\right)\right] \boldsymbol{\psi}_i = \mathbf{0} \tag{17}$$

The two projections are compared to the direct frequency response on Figure 5. The 48 first real undamped modes and a static correction are considered in the first basis. In the enriched basis, on addition to the static correction, the 24 first real undamped modes and the 24 first real modes associated with a shear modulus evaluated at the frequency $f_c = 200$Hz are taken. Figure 5 shows that the first reduction leads to overestimated damping and underestimated amplitudes and that the enrichment made in the second reduction gives a more accurate response.

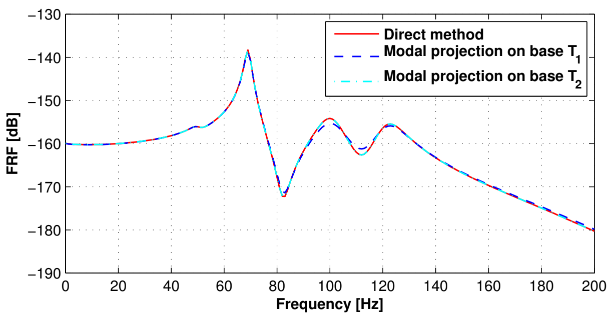

Figure 5: Frequency response of the damped structure by a direct method, a modal projection of Eq.8 on basis $\mathbf{T}_1 = [\boldsymbol{\phi}_{1..48}\ , \mathbf{T}_S]$ and a modal projection of Eq.8 on basis $\mathbf{T}_2 = [\boldsymbol{\phi}_{1..24}\ , \boldsymbol{\psi}_{1..24}(f_c = 200\text{Hz})\ , \mathbf{T}_S]$

3.2 Component mode synthesis

Component synthesis method is a substructuring coupling method for which the structure is divided into components. For each component i, the degrees of freedom $\mathbf{u}^i$ are divided into interface degrees of freedom $\mathbf{u}^i_J$ and internal degrees of freedom $\mathbf{u}^i_{\bar{J}}$. The interface degrees of freedom are considered as unknowns and the internal degrees of freedom are reduced using a reduction basis $\mathbf{T}$: $\mathbf{u}^i_{\bar{J}} = \mathbf{T}\mathbf{q}^i_{\bar{J}}$. By imposing continuity along component interfaces, components are coupled and the dynamic behaviour of the overall structure can be calculated from the resolution of a reduced system whose degrees of freedom are $\mathbf{q} = [\cup_i(\mathbf{u}^i_J), \cup_i(\mathbf{q}^i_{\bar{J}})]$.

The Craig-Bampton method is a reduction method commonly used to reduce the internal degrees of freedom in model substructuring. The Craig-Bampton reduction basis, in the first level of approximation, consists of low frequency fixed-interface normal modes $(\boldsymbol{\phi}_i)$ and a static condensation $\mathbf{T}_s$:

$$\mathbf{T}_{CB} = [(\boldsymbol{\phi}_i)\ ,\ \mathbf{T}_s] \tag{18}$$

where $(\boldsymbol{\phi}_i)$ are real undamped fixed-interface modes of the component solutions of

$$\left(\mathbf{K}^0_{S,\bar{J}\bar{J}} - \omega_i^2 \left(\mathbf{M}_{S,\bar{J}\bar{J}} + \mathbf{M}^a_{S,\bar{J}\bar{J}}\right)\right) \boldsymbol{\phi}_i = \mathbf{0}, \tag{19}$$

and the static condensation $\mathbf{T}_s$ corresponds to the static response of the internal degrees of freedom to imposed unit displacements on the interface degrees of freedom

$$[\mathbf{u}_J, \mathbf{u}_{\bar{J}}]^T = \mathbf{T}_s \mathbf{u}_J = [\mathbf{I}, -\mathbf{K}^{-1}_{\bar{J}\bar{J}_{|(\omega=\omega_c)}} \mathbf{K}_{\bar{J}J}]^T \mathbf{u}_J \tag{20}$$

The structure of Figure 1 is divided into two substructures. The first corresponds to the ring with partial viscoelastic core and the external fluid, and the second to the stiffeners (Figure 6).

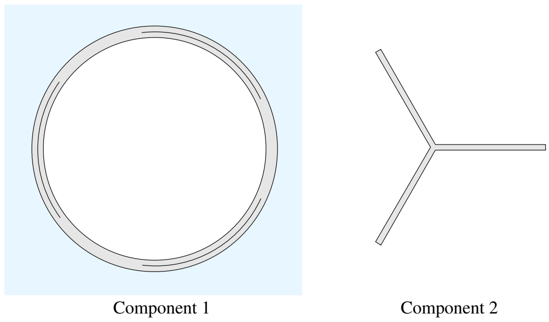

Figure 6: Substructuring of the structure

The component mode synthesis is applied to the substructuring of Figure 6. The first 24 real undamped modes are taken for each component. The frequency response function of the structure calculated from this method is compared to the frequency responses obtained by a direct method and by a modal projection without enrichment on Figure 7.

The component mode synthesis gives similar results to the modal projection on a basis without enrichment which is expected as for both methods, only real undamped modes are considered. An analogy between the modal projection and the component mode synthesis leads to enrich the Craig-Bampton reduction basis with fixed-interface modes calculated for a high frequency modulus. This enriched component mode synthesis is compared to the direct method and to the enriched modal projection on Figure 8, and proves to be efficient to predict the frequency behaviour of the damped structure.

Table 1 gives the comparisons of the different methods in terms of normalized computation time of the frequency response function, precision with respect to the direct solution and size of the reduced model to be solved. The error is

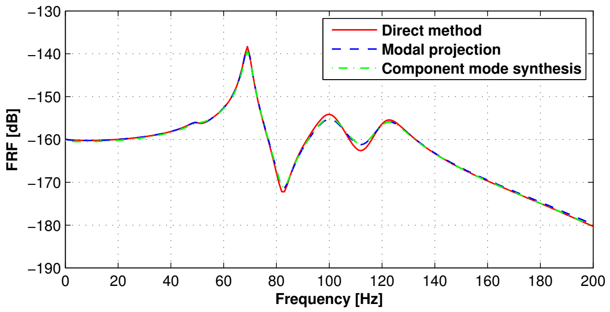

Figure 7: Frequency response of the damped structure by a direct method, a modal projection of Eq.8 on basis $\mathbf{T}_1 = [\boldsymbol{\phi}_{1..48}\,, \mathbf{T}_S]$ and a component mode synthesis applied to the substructuring described on Figure 6 with 24 modes per component.

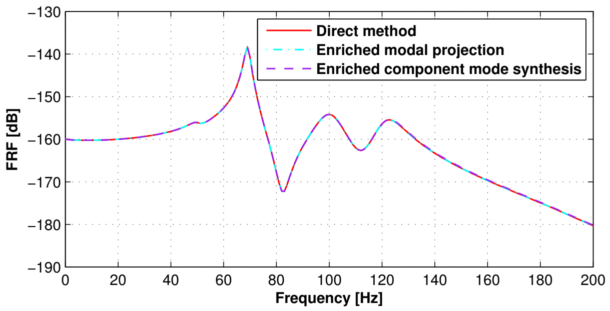

Figure 8: Frequency response of the damped structure by a direct method, a modal projection of Eq.8 on basis $\mathbf{T}_2 = [\boldsymbol{\phi}_{1..24}\,, \boldsymbol{\psi}_{1..24}(f_c = 200\text{Hz})\,, \mathbf{T}_S]$ and an enriched component mode synthesis applied to the substructuring described on Figure 6 with 12 real undamped fixed-interface modes and 12 fixed-interface modes calulated with a shear modulus evaluated at the frequency $f_c = 200$Hz per component.

evaluated as follows:

$$\epsilon(F) = 100 \int_{\omega_{\min}}^{\omega_{\max}} \left(\frac{F(\omega) - F_{\text{ref}}(\omega)}{F_{\text{ref}}(\omega)} \right)^2 \mathrm{d}\omega \qquad (21)$$

where F_{ref} is the direct frequency response function and F is the frequency response function evaluated by a reduced method.

The component modes synthesis allows easy parallelization of the calculation of component's modes, and is expected to be more efficient than the modal projection method for structures with a high number of degrees of freedom.

4 Extension to a tridimensional structure

The enriched modal projection proposed in the previous section is applied to the tridimensional structure represented on Figure 9. The structure is made of steel and a viscoelastic layer (thickness 5 mm) of Deltane 350 is introduced at the core of the cylindrical shell. The diameter of the structure is about 4 m, while the thickness is of the order of 0.2 m. The boundary conditions and load are similar to the ones applied to the bidimensional structure. The mesh is composed of 35000 quadratic tetrahedra, which represents about 80000 degrees of freedom. As a first approach, in order to test the efficiency and accuracy of the proposed reduced method, the fluid is not taken into account.

Table 1: Comparison of reduction methods.

	Computational time (%)	Error (%)	Size of reduced model
Direct method	100	-	-
Modal projection	2.5	3.5	(48×48)
Enriched modal projection	2.8	10^{-5}	(48×48)
Component mode synthesis	3.5	3.8	(64×64)
Enriched component mode synthesis	3.5	0.8	(64×64)

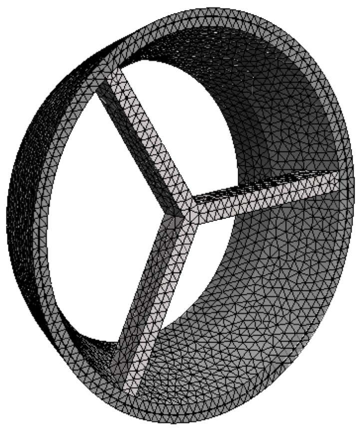

Figure 9: Tridimensional structure studied.

The constitutive behavior implemented is that of Hooke's law for which the stresses and strains have been separated into spheric (subscript s) and deviatoric (subscript d) parts :

$$\boldsymbol{\sigma} = \mathbf{C}\boldsymbol{\epsilon} \qquad (22)$$

where $\mathbf{C} = K\mathbf{C}_s + G\mathbf{C}_d$ with K the bulk modulus, G the shear modulus, $\mathbf{C}_s = [\underline{\mathbf{1}} \otimes \underline{\mathbf{1}}]$ and $\mathbf{C}_d = 2[\mathbf{I} - \frac{1}{3}(\underline{\mathbf{1}} \otimes \underline{\mathbf{1}})]$. $\underline{\mathbf{1}}$ and $\mathbf{I}$ denotes the second and the fourth order unit tensor respectively, in Voigt notation. The behavior law allows to consider frequency dependent shear and bulk moduli. In this study, the bulk modulus is real and constant, $K =$, and the shear modulus follows the fractional derivative model described in the first section.

The frequency response function of the structure is calculated with a direct method, and compared to the one obtained with the proposed reduced method for varying number of modes used in the reduction basis. The modes ψ_i of the enriched basis and the static correction are evaluated at a modulus calculated at 200 Hz. Figure 10 and Table 2 show that the enriched modal projection gives accurate results. The last column of Table 2 gives the ratio between the maximum eigenfrequency $max(f_i)$ of the modes ψ_i taken in the reduction basis to the maximum of the frequency range investigated f_{max}. The computational time of the frequency response function is reduced by a ratio of about 60 when using a reduced basis. The deformed shape of the structure at 197 Hz is shown on Figure 11.

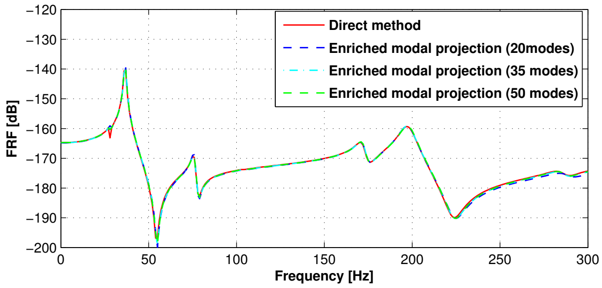

Figure 10: Frequency response function of the structure calculated from a direct method and an enriched modal projection using 20, 35 and 50 modes ϕ_i and ψ_i.

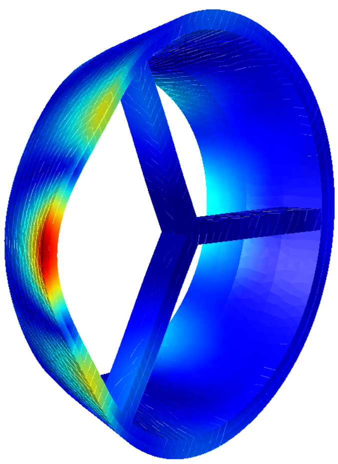

Figure 11: Deformed shape of the structure at 197 Hz.

Table 2: Convergence of the enriched modal projection method.

Number of modes	Error (%)	$\frac{max(f_i)}{f_{max}}$
20	5.9	1
35	4.0	1.5
50	3.6	2

5 Conclusion

This works presents a methodology to solve viscoelastically damped vibroacoustic problems. The enrichment of the modal projection basis or the Craig-Bampton basis applied to a water-immersed ring viscoelastically treated proved to be an efficient method to predict the vibrations of the structure and the pressure level in the fluid at low cost.
Remaining efforts concern the application of the component mode synthesis to a tridimensional structure coupled to fluid. A more thoroughly study of the experimental identification of viscoelastic materials properties is under progress.

Acknowledgments

The financial support of the DGA/MRIS(Mission for Scientific Research and Innovation) and the DCNS is gratefully acknowledged.

References

[1] A.C. Galucio, J.-F. Deü, R. Ohayon, ”Finite element formulation of viscoelastic sandwich beams using fractional derivative operators”, *Computational Mechanics* **33**, 282-291 (2004)

[2] M.A. Trindade, A. Benjeddou, R. Ohayon, ”Finite element modelling of hybrid active-passive vibrations damping of multilayer piezoelectric sandwich beams-part I: formulation; part II: system analysis”, *International Journal for Numerical Methods in Engineering* **51**, 835-864 (2001)

[3] L. Rouleau, J.-F. Deü, A. Legay, J.-F. Sigrist, ”Vibroacoustic study of a viscoelastic sandwich ring immersed in water”, *Journal of Sound and Vibration*, **331**, 522-539 (2012)

[4] A.-S. Plouin, E. Balmès, ”Steel/viscoelastic/steel sandwich shells. Computational methods and experimental validations”, *International Modal Analysis Conference*, San Antonio (2000)